

*Gravitational form factor and
D-term of hydrogen-like atoms in
QED*

Yizhuang Liu, Jagiellonian University

Excited QCD 2022

The talk is based on the recent work with Xiangdong-Ji:

Gravitational Tensor-Monopole Moment of Hydrogen Atom To Order $O(\alpha)$.

Arxiv: 2208.05029.

Outline

- Energy Momentum Tensor and mass distribution of bound-states.
- EMT form-factor for hydrogen-like atom: scale separation, IR sensitivity and NRQED.
- EMT form-factor in NRQED.
- Results and discussion.

Energy Momentum Tensor (EMT)

- Energy-momentum tensor (EMT) is not an unfamiliar object .
 1. $T^{\mu\nu}(x)$ describes the distribution of mass and momentum flow in many systems. Such as:
 - Classical continuum matter. σ^{ij} called stress tensor. Often decomposed further into **pressure** (trace) and **shear-force** (traceless).
 - Classical electromagnetic dynamics. T^{0i} is the famous **Poynting vector**. T^{ij} is the famous **Maxwell stress tensor**.

EMT in QFT.

- In QFT, $T^{\mu\nu}(x)$ is more subtle.
 1. Formally as Noether's currents of space-time translation symmetry.
 2. $T^{00}(x)$: the energy density. $T^{0i}(x)$ the momentum density.
 $T^{ij}(x)$: momentum current density. $\partial_\mu T^{\mu\nu} = 0$.
 3. Ambiguity exists. Even for the "canonical" one, explicit construction differs in regularization schemes. *Meaning: DR vs Lattice vs Pauli-Vilas, the same renormalized $T^{\mu\nu}$ looks quite different in terms of bare operators.*

Canonical EMT in practical QFT

- The canonical EMT for gauge theory (QED or QCD) in **DR**.

1. $T^{\mu\nu} = -F^{\mu\rho} F_{\rho}^{\nu} + \frac{1}{4} g^{\mu\nu} F^2 + \bar{\psi} i \gamma^{(\mu} D^{\nu)} \psi.$

2. **Gluon** and **quark** parts are **not** RG invariant by themselves.

3. $T^{\mu\nu} = T_{twist-2}^{\mu\nu} + \frac{g^{\mu\nu}}{4-2\epsilon} \left(m \bar{\psi} \psi - \frac{2\epsilon}{4-2\epsilon} F^2 \right)$ decomposed into **traceless** and **trace-full** parts.

4. $T_{\mu}^{\mu} = m \bar{\psi} \psi + \left(\frac{\beta}{2g} F^2 + m \gamma_m \bar{\psi} \psi \right).$ The **trace-anomaly**.

5. $T^{00}(x)$: mass decomposition. Ambiguity & scheme & scale.

Hadronic EMT form factor.

- The EMT form factor of spin- $\frac{1}{2}$ particle ($q = P' - P, \bar{P} = \frac{P+P'}{2}$)
- $\langle P' | T^{\mu\nu} | P \rangle =$
$$\bar{u}(P') \left(A(q) \gamma^{(\mu} \bar{P}^{\nu)} + B(q) \frac{\bar{P}^{(\mu} i \sigma^{\nu)\alpha} q_{\alpha}}{2M} + C(q) (q^{\mu} q^{\nu} - g^{\mu\nu} q^2) \right) u(P)$$
- 1. The **Mass**, **Spin** form factors. $A(0) = B(0) = 1$. Mass and spin sum-rule.
- 2. What about **$C(0)$** ? This is called the **D-term** and remains unknown.
- 3. Is **$C(0)$** always **negative due to stability**?

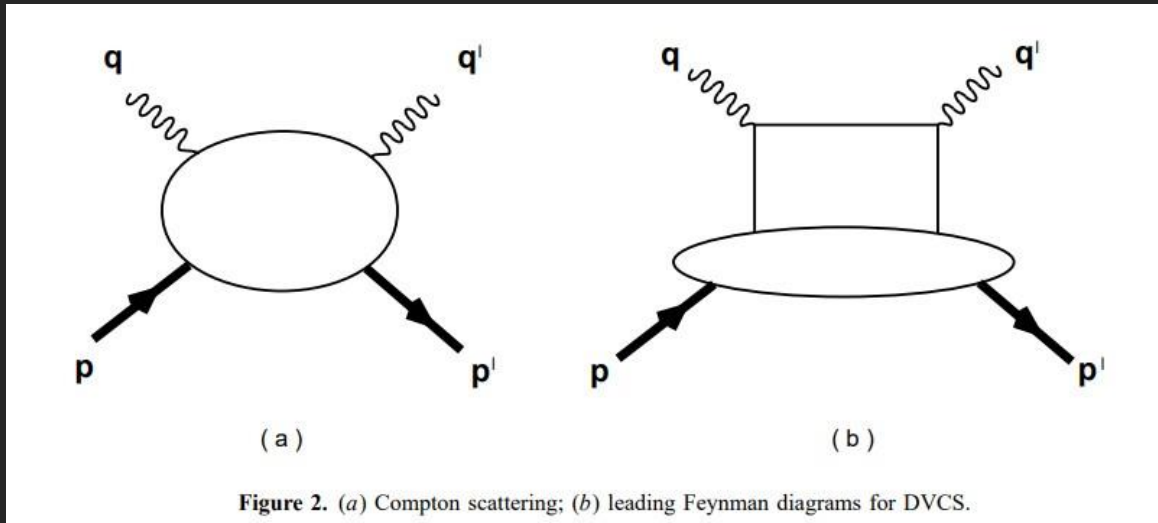
Hadronic EMT form factor and GPDs

hep-ph/9609381, Ji
hep-ph/9807358, Ji
hep-ph/0307382, Diehl

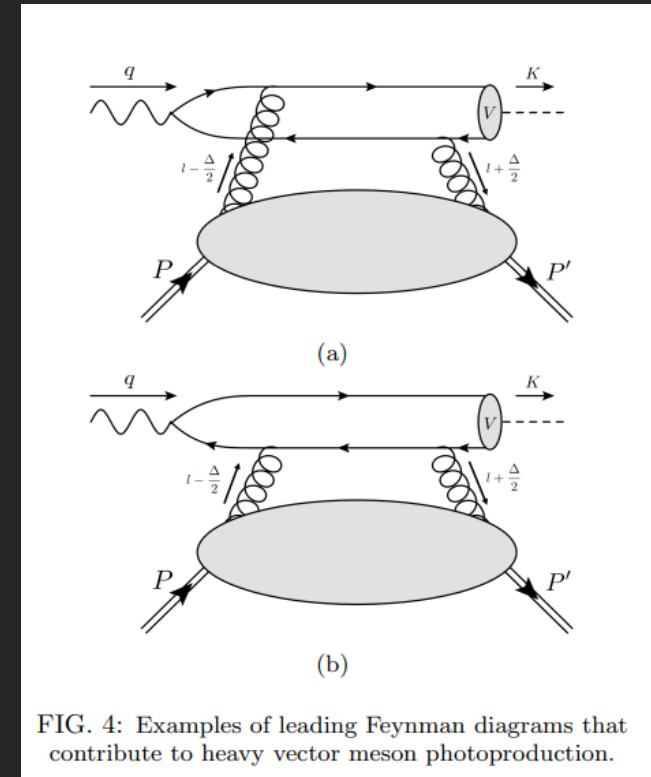
- Where the EMT form factor can be probed ?
 1. Twist-two parts. First moment of the **Generalized parton distributions** (GPD). $F(x, \xi, q) \sim H + E$.
 2. $\int_{-1}^1 x H_g(x, \xi, q) = A_g(q) + (2\xi)^2 C_g(q)$,
 $\int_{-1}^1 x E_g(x, \xi, q) = A_g(q) - (2\xi)^2 C_g(q)$. And similar for quark.
 3. Can be probed in DVCS, where $\xi = -\frac{q^+}{2\bar{P}^+}$ is called the skewness.
 4. Near threshold J/ψ production: Clue to $C(0)$?

PhysRevD.103.096010, Guo, Ji, Liu
PhysRevD.106.086004, Mamo&Zahed

DVCS and vector meson production



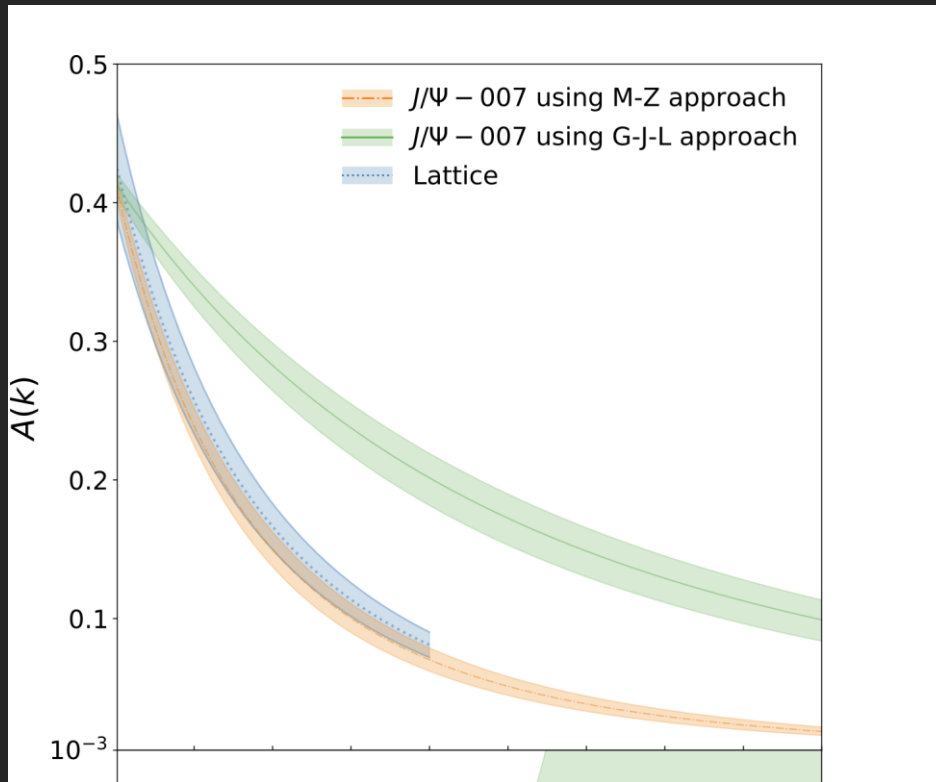
In the Bjorken limit, the DVCS amplitudes factorizes into GPDs and Hard kernels.



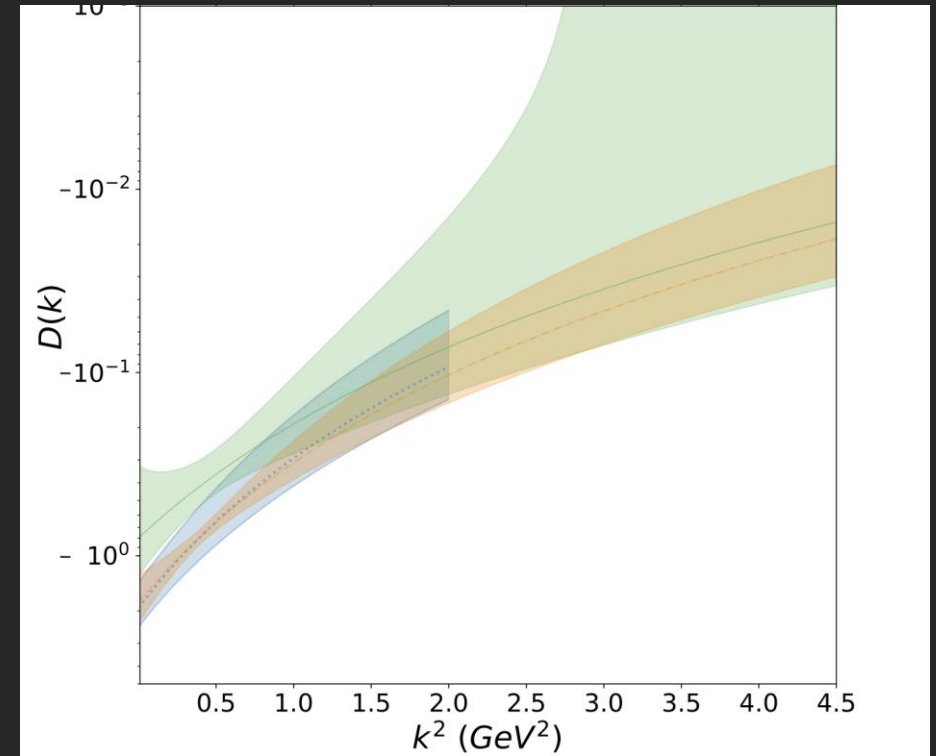
The vector meson production can also be used to probe GPDs. Near threshold may probe $\xi \sim 1$ region.

Threshold J/Ψ production and EMT form factor

Experiment
performed in
J-lab.
2207.05212



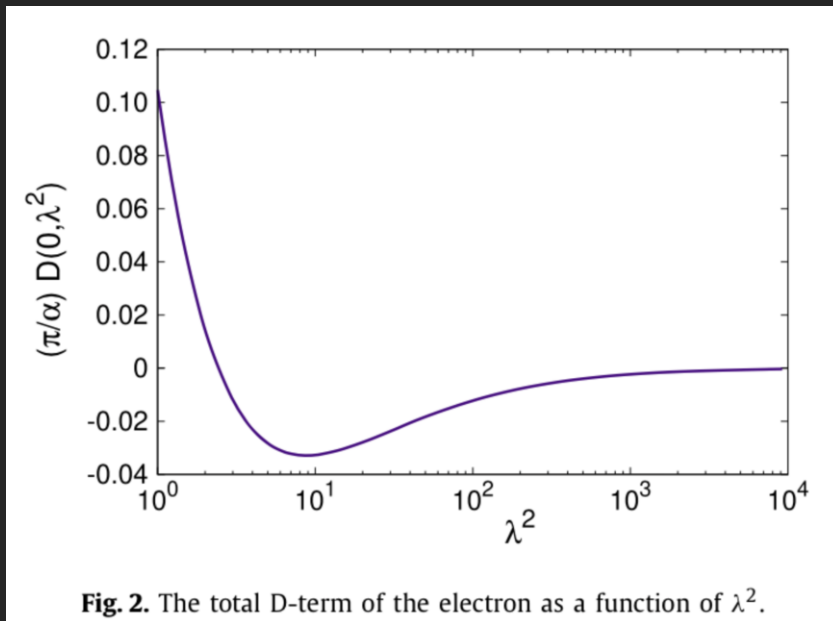
Extraction of the proton A form factor based on various approaches vs Lattice.



Extraction of the proton $D = 4C$ form factor.

EMT form factor and Sign of $C(0)$: clue from QED?

- Despite progress, uncertainty still large for $C(0)$ and its physical meaning. Is $C(0)$ always **negative due to stability?** hep-ph/9902451, Polyakov&Weiss
- Insights from QED will be helpful.
- The C-form factor for single electron has been used as an example.



The D-term of single electron is **negative** for small photon mass.

Figure from Metz&Pasquini&Rodini

Phys.Lett.B 820 (2021) 136501,
Metz&Pasquini&Rodini
Phys. Rev. D 15 (1977) 538, Milton,

However, **single electron is not bound state.**

But hydrogen atom is.

Outline

- Energy Momentum Tensor and mass distribution of bound-states.
- EMT form-factor for hydrogen-like atom: scale separation, IR sensitivity and NRQED.
- EMT form-factor in NRQED.
- Results and discussion.

Bound states in QED: the microscopic theory

- The most famous bound state in QFT: the hydrogen atom.
- Field theoretical approach: heavy proton / **dressed-Dirac theory**.
 1. $\mathcal{L} = \bar{N}iD^0N + \mathcal{L}_{QED}$. Bethe-Salpeter approach.
 2. $\mathcal{L} = -e\bar{\psi}\gamma^\mu\psi\mathcal{A}_\mu + \mathcal{L}_{QED}$. $\mathcal{A}^\mu = \frac{e}{4\pi|\vec{r}|}\delta^{\mu,0}$: the static Coulomb field of the proton.
 3. Can be shown to be equivalent.

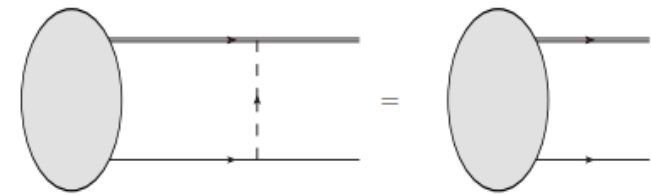


FIG. 1: The Bethe-Salpeter equation for the wave function Φ denoted by the oval blob. Double line represents propagator of proton field and single line represents the electron propagator. The dashed line represents the exchange of a Coulomb photon.

Bound states in QED: the microscopic theory

4. Renormalized using the same $Z_1 = Z_2$ and Z_3 as the free QED.

$$\begin{aligned} \delta\mathcal{L} = & (Z_1 - 1)\bar{\psi}_R(i\gamma \cdot \partial - m)\psi_R - e(Z_1 - 1)\bar{\psi}_R\gamma^\mu\psi(A_{\mu,R} + \mathcal{A}_\mu) \\ & - \delta_m m Z_1 \bar{\psi}_R\psi_R - \frac{Z_3 - 1}{4} F_R^{\mu\nu} F_{\mu\nu,R} - \frac{Z_3 - 1}{2} F_R^{\mu\nu} \mathcal{F}_{\mu\nu} , \end{aligned}$$

5. The free theory defined by the complete set of solutions of Dirac equation in the background field.
6. Radiative correction added perturbatively in terms of standard Feynman rules. Main difference: the **Coulomb-Dirac propagator**.

Bound states in QED: the microscopic theory

4. Example: self-energy correction to bound-state.

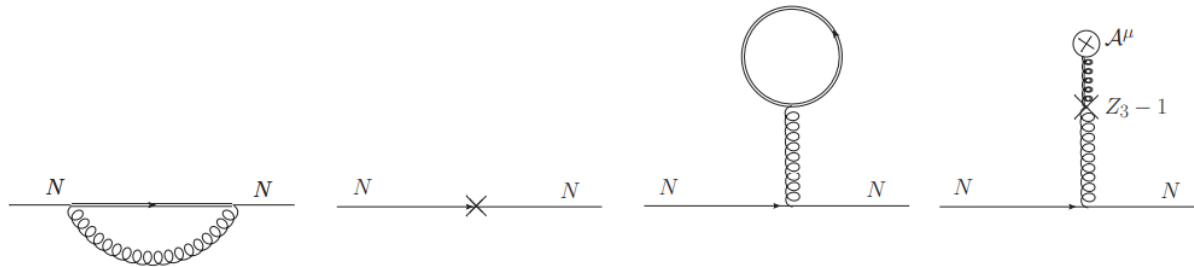


Figure 4: The Feynman diagram for the one-loop electron self energy. The double lines are dressed electron propagators and the crosses are counter terms. They contribute to the energy shift δE_N . Notice that the fourth diagram corresponds to the counter term $\frac{Z_3-1}{2} F^{\mu\nu} F_{\mu\nu}$ that couples the background and radiative photon fields.

5. In general, analytic calculation is very difficult.

Scale separation and NRQED

- However, when $\alpha \ll 1$, simplification occurs due to the **emergent scale separation** of the bound states:
 1. The **soft scale** $k_s \sim \alpha m_e$. The size of the NR wave function.
 2. The **ultra-soft scale** $k_{us} \sim \alpha^2 m_e$. The binding energy/kinematic energy.
 3. The **UV scale** m_e . The electron mass.
- When expanded in the scale separations $\frac{\alpha m_e}{m_e}$ or $\frac{\alpha^2 m_e}{m_e}$, expression simplifies a lot. **Power & log** in renormalizable theory.
- Similar in spirit to twist expansion/OPE in high-energy limit.

Scale separation and NRQED

- The NRQED is the modern way to organize this expansion .
One needs

1. NRQED Lagrangian in terms of **effective fields**:

$$\mathcal{L} = \Psi^\dagger \left(iD^0 + \frac{\vec{D}^2}{2m} - \frac{c_F e}{2m} \vec{\sigma} \cdot \vec{B} \right) \Psi - \frac{1}{4} F^2 + \mathcal{O}\left(\frac{1}{m^2}\right)$$

2. The **matching coefficients** c_F and others matches the **UV of IR to the IR of UV**. “Splitting of Logarithms”.
3. For individual operators, matching through local counter-terms.

EMT for NRQED

- One can construct the “tree-level” EMT in NRQED:

$$T_{\text{tree}}^{ij} = T_e^{ij} + T_\gamma^{ij} + T_{\gamma p}^{ij} + T_p^{ij}$$

1. $T_e^{ij} = -\frac{1}{4m} \Psi^\dagger D^i D^j \Psi - \frac{1}{4m} D^i D^j \Psi^\dagger \Psi + \frac{1}{8m} (D^{(i} \Psi)^\dagger D^{j)} \Psi.$

2. T_γ^{ij} is the standard photon EMT.

3. $T_{\gamma p}^{ij} = \delta^{ij} \nabla V_p \cdot \nabla V_e - \partial^i V_p \partial^j V_e - \partial^j V_p \partial^i V_e$ is the interference between the Coulomb fields of electron and proton.

4. $\nabla^2 V_e = e \Psi^\dagger \Psi$ is the Coulomb field of the electron. $V_p = \frac{e}{4\pi r}.$

EMT for NRQED

5. One can show that the above T_{tree}^{ij} is **conserved in symmetric bound-states** using EOM.
6. However, to match to the T^{ij} in QED, local counter-terms are required.
 - In this work we calculate to order $\frac{\alpha}{m}$. At this order, one needs only one counter-term

$$T_{NRQED}^{ij} = T_{tree}^{ij} + d_0(\partial^i \partial^j - \delta^{ij} \partial^2) \psi^\dagger \psi + \mathcal{O}\left(\frac{\alpha}{m^2}\right).$$

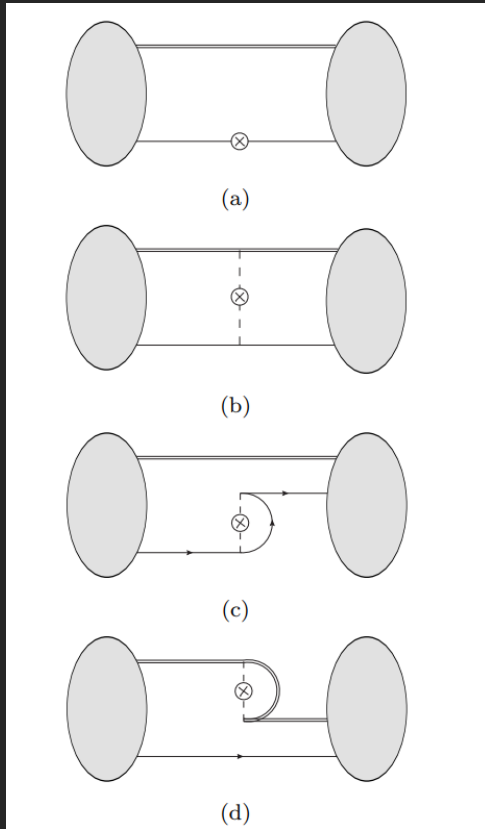
The overall-strategy of the calculation.

1. To obtain the matching coefficient d_0 . One calculates using **Free-NRQED** and match to QED.

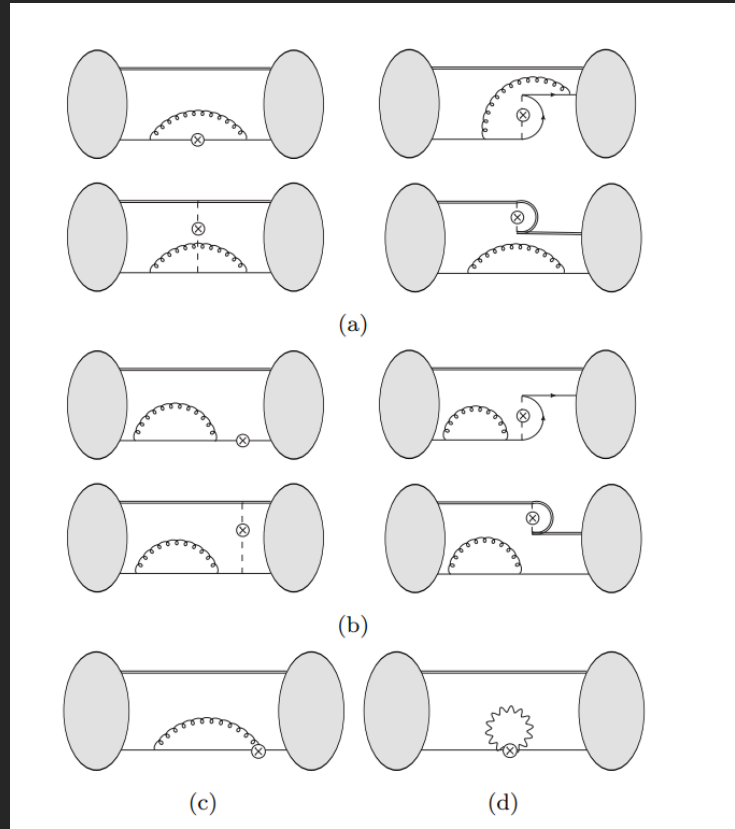
Reason: Free NRQED and dressed NRQED shares the same UV.

2. Combine d_0 with bound-state calculation to get full result.
3. DR with $D = 3 - 2\epsilon$ is adopted consistently. Coulomb gauge is chosen.
4. **Power-counting in α** eliminates all the fermionic diagrams.

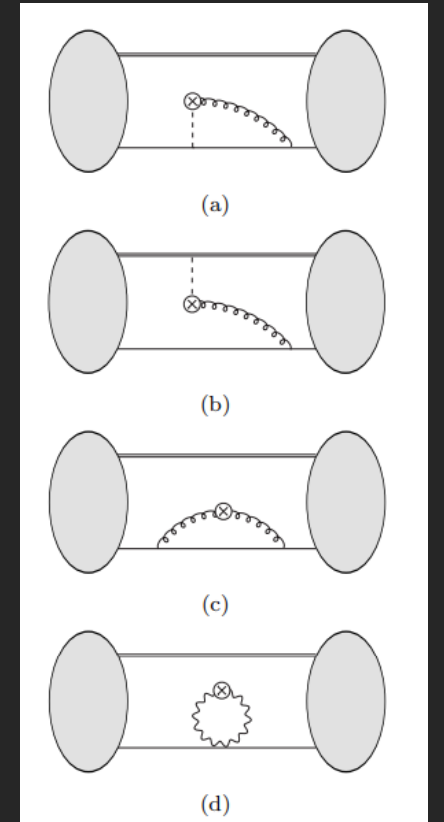
The overall-strategy of the calculation.



The leading order diagrams.



The one-loop fermionic diagrams.



The photonic diagrams.

The overall-strategy of the calculation.

- An example of power-counting in α

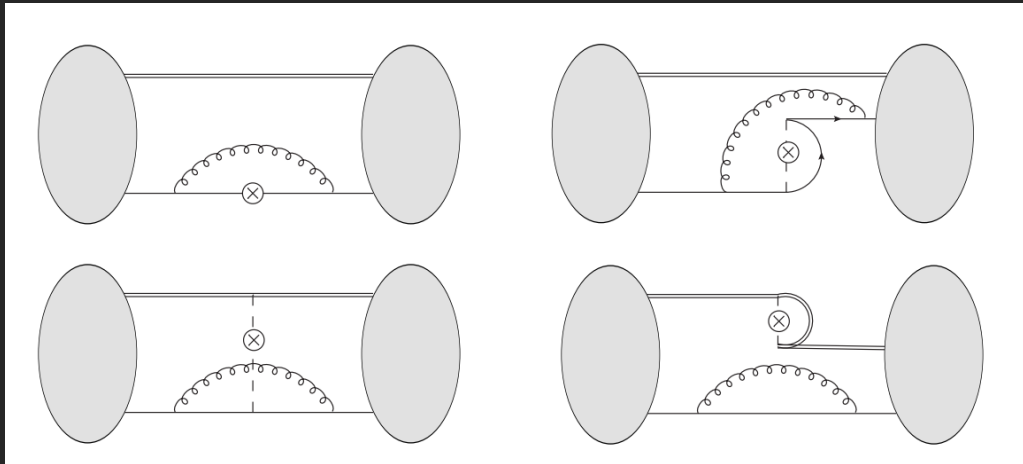


Fig. (6a) in 2208.05029

$$\langle T_0^{ij} \rangle_{6a}(\vec{q}) = e^2 \mu^{2\epsilon} \sum_{M, M'} \int \frac{d^D \vec{k}}{(2\pi)^D} \frac{(1 - \frac{1}{D}) \vec{v}_{0M'}(\vec{k}) \cdot \vec{v}_{M0}(\vec{k})}{(E_0 - |\vec{k}| - E_M)(E_0 - |\vec{k}| - E_{M'}) 2|\vec{k}|} \langle M' | T_0^{ij}(\vec{q}) | M \rangle, \quad (64)$$

where the $T_0^{ij}(\vec{q})$ is defined in Eq. (62), including the proton part when $M = M'$. It is easy to see that for $D = 3$, when $|\vec{k}| = \mathcal{O}(\alpha m_e)$ or $|\vec{k}| = \mathcal{O}(\alpha^2 m_e)$, the two energy denominators and one phase-space measure $2|\vec{k}|$ for the photon contributes to $(\alpha m_e)^{-3}$ or $(\alpha m_e)^{-6}$, which is always canceled by the integration measure $\int d^3 \vec{k} = (\alpha m_e)^3$ or $(\alpha m_e)^6$, respectively. The two form-factors for the velocity operators will contribute to α^2 , while the matrix element $\langle M' | T_0^{ij}(q) | M \rangle$ as shown above will contribute to $\mathcal{O}(\alpha^2)$ at order $\mathcal{O}(q^0)$ and $\mathcal{O}(1)$ to $\mathcal{O}(q^2)$. Therefore, together with the overall e^2 , Fig. 6a will contribute at order $\mathcal{O}(\alpha^3)$ to the coefficients of q^2 , and to $\mathcal{O}(\alpha^5)$ for coefficients of q^0 , therefore not relevant for our calculation. Similar argument can be used to show that diagrams in Fig. 6b and Fig. 6c (T_{e1}^{ij}) will be irrelevant to NLO as well. The last diagram Fig. 6d,

The overall-strategy of the calculation.

- DR for bound states.
 1. All quantities are in D dimensions, including NR wave functions.
 2. However, the sum-rule $\sum_M \frac{2\vec{v}_{NM}\cdot\vec{v}_{MN}}{D(E_M-E_N)} = \frac{1}{m}$ will guarantee that the coefficients of the $\frac{1}{\epsilon}$ poles are D -independent constants.
 3. Similar to the simplified calculation to the Lamb' shift.

Caswell/Lepage, Phys. Lett. B 167, 437.
Labelle, Phys. Rev. D 58, 093013.
Pineda and Soto, Nucl. Phys. B Proc. Suppl.
64,428

Outline

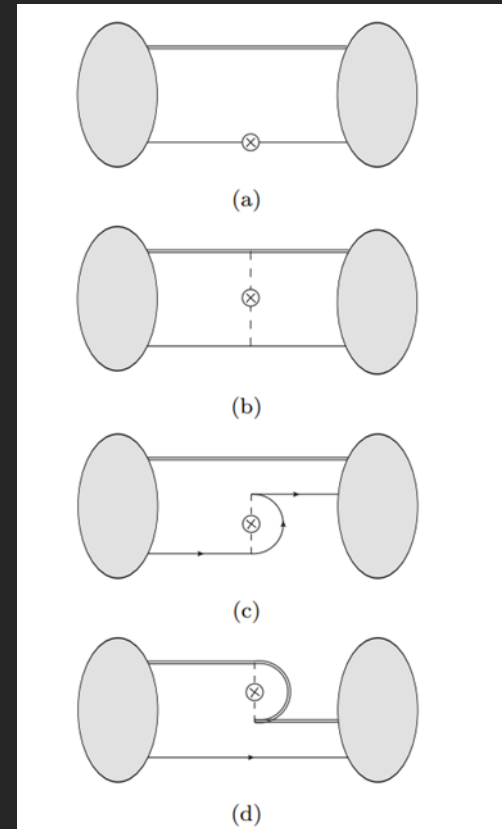
- Energy Momentum Tensor and mass distribution of bound-states.
- EMT form-factor for hydrogen-like atom: scale separation, IR sensitivity and NRQED.
- EMT form-factor in NRQED.
- Results and discussion.

The Leading order results

- $$\langle 0 | T^{ij}(q) | 0 \rangle_H = (q^i q^j - \delta^{ij} q^2) \frac{C_H(q)}{m_e}$$

$$\begin{aligned} \frac{C_H(q)}{m_e} = & \frac{1}{2m_e \left(\frac{q^2}{\alpha^2 m_e^2} + 4 \right)} - \frac{\alpha}{4|q|} \left(\frac{\pi}{2} - \text{Arctan} \frac{q}{2\alpha m_e} \right) \\ & + \frac{\alpha\pi}{|q|} \frac{1}{\left(\frac{q^2}{\alpha^2 m_e^2} + 4 \right)^2} + \frac{\alpha\pi}{|q|} \frac{1}{\left(\frac{q^2}{\alpha^2 M^2} + 4 \right)^2}. \end{aligned}$$

- $$\frac{C_H(0)}{m_e} = \frac{1}{4m_e} \text{ is positive.}$$



The leading order diagrams.

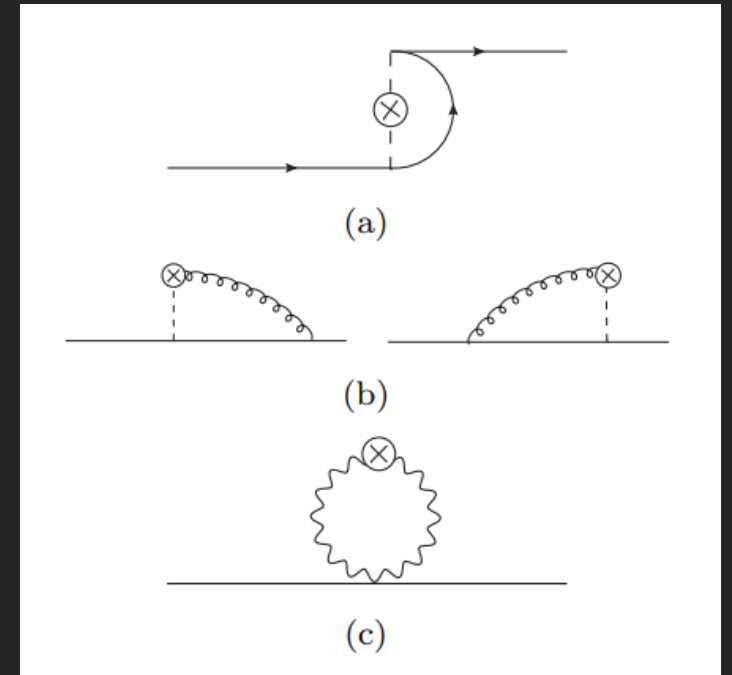
The matching coefficients d_0

$$T_{NRQED}^{ij} = T_{tree}^{ij} + d_0(\partial^i \partial^j - \delta^{ij} \partial^2) \psi^\dagger \psi$$

- The condition for matching

$$\langle \vec{Q} | T_{NRQED}^{ij} | -\vec{Q} \rangle = \langle \vec{Q} | T_{QED}^{ij} | -\vec{Q} \rangle$$

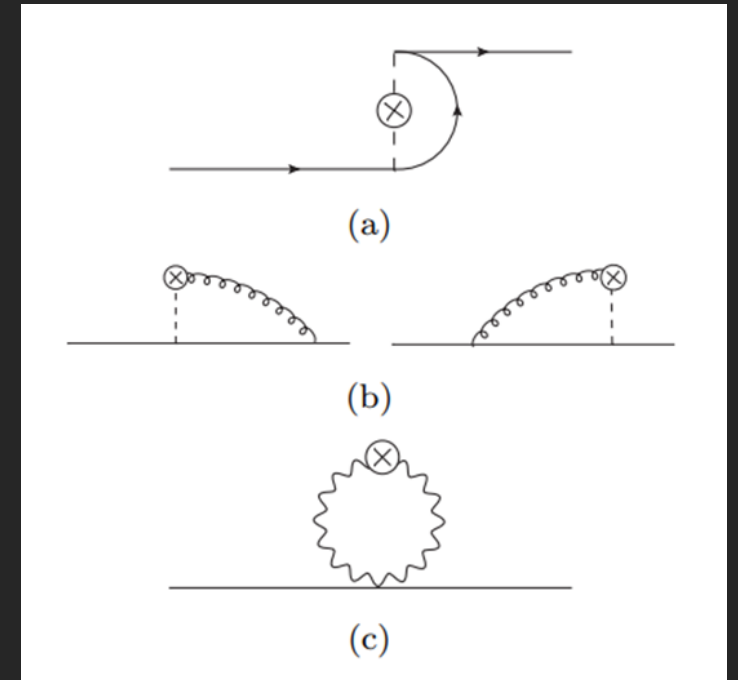
- Only photonic diagrams are relevant.
- Coulomb-self, mixed and tadpole diagram.
- Tadpole diagram originates from backward moving diagram in QED.



The relevant diagrams in free NRQED for T_{tree}^{ij} .

The matching coefficients d_0

- T^{ii} (trace) and $Q^i T^{ij} Q^j$ (longitudinal) calculated separately.
1. The Coulomb-self diagram is conserved separately.
 2. Longitudinal parts cancel between the mixed and tadpole diagrams.
 3. T^{ii} of the mixed diagram contains the logarithm.



The relevant diagrams in free NRQED.

The matching coefficients d_0

- The total results reads

$$\langle T_{\text{tree}}^{ij} \rangle(2\vec{Q}) = (Q^i Q^j - \delta^{ij} Q^2) \tilde{C}(Q^2), \quad (97)$$

where

$$\tilde{C}(Q^2) = \frac{\alpha\pi}{8|Q|} + \frac{e^2}{6m_e\pi^2} \left(-\frac{1}{\epsilon} + \ln \frac{Q^2}{\mu^2} + \gamma_E - \ln \pi - \frac{7}{6} \right). \quad (98)$$

- Same in IR with QED, differs in UV

$$\tilde{C}_{\text{QED}}(Q^2) = \frac{\alpha\pi}{8|Q|} + \frac{e^2}{6m_e\pi^2} \ln \frac{4Q^2}{m_e^2} - \frac{11e^2}{72m_e\pi^2} \quad (99)$$

The matching coefficients d_0

- As a result, one obtains the d_0

$$d_0 = -\frac{\alpha}{6\pi m_e} \left(\frac{1}{\epsilon} + \ln \frac{4\mu^2}{m_e^2} + \ln \pi - \gamma_E + \frac{1}{4} \right). \quad (101)$$

- It contains UV logarithms $\ln \frac{\mu^2}{m_e^2}$, but no IR sensitivity.

The NLO contribution for bound-state.

Figure (b) vanishes.

- For the bound-state, the **pure-radiative diagram is activated** in the ultra-soft region.
- Dipoles expansion performed in ultra-soft region as usual.
- Tadpole diagram remains the same as Free-NRQED.
- Cancellation of longitudinal parts between (a), (c) and (d).

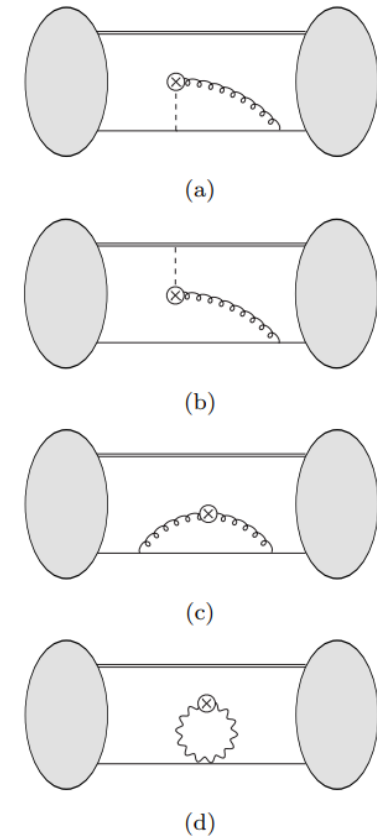


FIG. 7: The order- $\mathcal{O}(\alpha)$ contributions to $T_{\gamma}^{ij} + T_{\gamma p}^{ij}$ for a bound state. Dashed lines represent Coulomb photons and crossed circles denote the operator insertions.

The NLO contribution: checking conservation.

- For Figure (a)

$$Q^i \langle T_{\gamma \parallel \perp}^{ij} \rangle_{7a} Q^j = \frac{Q^4 e^2}{\pi^2} \sum_M \frac{2\vec{v}_{M0} \cdot \vec{v}_{0M}}{D(E_M - E_0)} \left(-\frac{1}{15\epsilon} + \frac{1}{15} \ln \frac{(E_M - E_0)^2}{\mu^2} + \frac{-15 \ln \pi + 15\gamma_E - 1}{225} \right).$$

- For Figure (c)

$$Q^i \langle T_{\gamma \perp}^{ij} \rangle_{7c} Q^j = \frac{Q^4 e^2}{\pi^2} \sum_M \frac{2\vec{v}_{0M} \cdot \vec{v}_{M0}}{D(E_M - E_0)} \left(\frac{1}{15} \ln \frac{Q^2}{(E_M - E_0)^2} + \frac{15 \ln 4 - 46}{225} \right).$$

- For Figure (d)

$$Q^i \langle T_{\gamma \perp}^{ij} \rangle_{7d} Q^j = \frac{e^2}{15m_e \pi^2 \epsilon} Q^4 + \frac{e^2}{15m_e \pi^2} Q^4 \left(-\ln \frac{Q^2}{\mu^2} + c'_2 \right),$$

$$c'_2 = \gamma_E - 3 + \ln 4 + \ln \pi + 2\psi \left(\frac{7}{2} \right) \equiv \frac{47}{15} - \gamma_E + \ln \pi - \ln 4.$$

Cancellation works!

The NLO contribution: The total results

- As a result, from T^{ii} one has

$$\langle T_{\text{tree}}^{ij} \rangle(2\vec{Q}) = (Q^i Q^j - \delta^{ij} Q^2) \tilde{C}_s(Q^2) ,$$

$$\tilde{C}_s(Q^2 = 0) = \frac{e^2}{6\pi^2} \sum_M \frac{2\vec{v}_{M0} \cdot \vec{v}_{0M}}{D(E_M - E_0)} \left(-\frac{1}{\epsilon} + \ln \frac{(E_M - E_0)^2}{\mu^2} + \gamma_E - \ln \pi - \frac{1}{2} \right) .$$

- To match to QED, simply adds $-4d_0$. This leads to our **result**.

Outline

- Energy Momentum Tensor and mass distribution of bound-states.
- EMT form-factor for hydrogen-like atom: scale separation, IR sensitivity and NRQED.
- EMT form-factor in NRQED.
- Results and discussion.

The NLO contribution: The total results

- The D-term for hydrogen-atom

$$1. \langle 0 | T^{ij}(q) | 0 \rangle_H = (q^i q^j - \delta^{ij} q^2) \frac{C_H(q)}{m_e}$$

$$2. \frac{C_H(0)}{m_e} = \tau_H = \frac{1}{4m_e} + \frac{\alpha}{6\pi} \sum_{M \neq 0} \frac{2\vec{v}_{0M} \cdot \vec{v}_{M0}}{D(E_M - E_0)} \left(\ln \frac{4(E_M - E_0)^2}{m_e^2} - \frac{1}{4} \right)$$

- The logarithm couples the UV and IR. Similar to the Bethe logarithm.
- Both continuum and discrete spectrum contributes.

The NLO contribution: The total results

- More explicitly, one has

$$\tau_H = \frac{1}{4m_e} + \frac{\alpha}{6\pi m_e} \left(\ln \alpha^2 + \tau_d + \tau_c - \frac{1}{4} \right)$$

- The **discrete spectrum** part

$$\tau_d = \sum_{n=2}^{\infty} \frac{2^8 n^5}{3(n^2 - 1)^4} \left(1 - \frac{2}{n+1}\right)^{2n} \ln \left(1 - \frac{1}{n^2}\right)^2 = -0.264 .$$

- The **continuum spectrum** part

$$\tau_c = \frac{1}{3} \int_0^{\infty} dE \frac{2^8 \ln(2E+1)^2}{(2E+1)^4} \frac{e^{-\frac{4}{\sqrt{2E}} \operatorname{Arccot}(\frac{1}{\sqrt{2E}})}}{1 - e^{-\frac{2\pi}{\sqrt{2E}}}} = 0.458 .$$

The NLO contribution: The total results

- Therefore, one has

$$\frac{\tau_H}{\tau_0} - 1 = \frac{4\alpha}{3\pi} (\ln \alpha - 0.028) = -1.54 \times 10^{-2}.$$

- The NLO contribution is **small** and **negative**.

Discussion and Summary

- The positivity of LO results is due to the long-range force in QED.
- Heuristically, one can guess it from result in free-QED

$$\tilde{C}_{\text{QED}}(Q^2) = \frac{\alpha\pi}{8|Q|} + \frac{e^2}{6m_e\pi^2} \ln \frac{4Q^2}{m_e^2} - \frac{11e^2}{72m_e\pi^2} \quad (99)$$

- At small Q , the natural IR cutoff now is αm_e , therefore LO positive while NLO negative.
- Positivity holds for small photon mass.

Discussion and Summary

- To summarize, the EMT form factor in QFT are important quantities to understand the mass-structure of bound-states.
- We use the hydrogen-like atom in QED as a non-trivial example to show that the D-term is not necessarily negative.
- The example is multi-scale in nature and demonstrates the basic principles of EFT.

Ambiguity in T^{00} -based mass sum-rules

2105.03974. Ji,
Liu, Schafer

- Consider the $O(N)$ non-linear sigma model in large N . One has
 1. The classical energy : $H_c = \frac{1}{2} \int dx ((\partial_t \pi^a)^2 + (\partial_x \pi^a)^2)$.
 2. The trace-anomaly : $H_a = \frac{\beta(g_0)}{2g_0} \int dx (\partial_\mu \pi^a)^2$.
 3. The true $H = \int dx T^{00}(x)$ looks different across schemes.

The contribution of H_c, H_a in different UV regularization schemes.

scheme	H_c	$H_a \equiv H_S$	H
$k^2 \leq \Lambda_{UV}^2$	$\frac{m}{2}$	$\frac{m}{2}$	m
lattice	$\frac{m}{2}$	$\frac{m}{2}$	m
$ k_1 \leq \Lambda_{UV}$	m	$\frac{m}{2}$	m
DR	m	$\frac{m}{2}$	m
$\frac{k_4^2}{\lambda^2} + k_1^2 \leq \Lambda_{UV}^2$	$\frac{\lambda m}{1+\lambda}$	$\frac{m}{2}$	m

The NLO contribution for bound-state.

- We use the
 1. Schwinger's α parameter for relativistic propagators
 2. The λ parameter for NR propagators
to disingularize all the Feynman integrals.
- Relations for Coulomb-gauge projections are used to simplify the integrand.
- Mellin transform trick is used to obtain the small q asymptotics.

The NLO contribution for bound-state.

- Typical parameter-space representation looks like

$$F_1(q) = -\frac{D}{4}\left(\frac{D}{2} + 1\right)\left(1 - \frac{1}{D}\right) \int_0^1 4x^2 \bar{x} dx \int_0^\infty d\lambda \int_0^1 dt_1 \int_0^1 dt_2 \int_0^\infty \rho^{-\frac{D}{2}+1} d\rho e^{-\frac{\lambda^2}{4} - \lambda\sqrt{\rho x t_1} - 4\rho x(1-x)t_2 q}, \quad (\text{E15})$$

$$F_2(q) = \frac{D}{2}\left(1 - \frac{1}{D}\right) \int_0^1 x(1 + 2x^2 - 2x) dx \int_0^\infty d\lambda \int_0^1 dt_1 \int_0^\infty \rho^{-\frac{D}{2}+1} d\rho e^{-\frac{\lambda^2}{4} - \lambda\sqrt{\rho x t_1} - 4\rho x(1-x)q}, \quad (\text{E16})$$

$$F_3(q) = -\frac{1}{D} \frac{D}{2} (1 - \epsilon) \int_0^1 4x(1-x) dx \int_0^\infty d\lambda \int_0^1 dt_1 \int_0^\infty \rho^{-\frac{D}{2}+1} d\rho e^{-\frac{\lambda^2}{4} - \lambda\sqrt{\rho} - 4\rho x(1-x)t_1 q}, \quad (\text{E17})$$

$$F_4(q) = (1 - \epsilon) \int_0^1 (2x - 1)^2 dx \int_0^\infty d\lambda \int_0^\infty \rho^{-\frac{D}{2}+1} d\rho e^{-\frac{\lambda^2}{4} - \lambda\sqrt{\rho} - 4\rho x(1-x)q}, \quad (\text{E18})$$

$$F_5(q) = -\frac{D}{2}\left(1 - \frac{1}{D}\right) \int_0^1 x(2x - 1) dx \int_0^\infty d\lambda \int_0^1 dt_1 \int_0^\infty \rho^{-\frac{D}{2}+1} d\rho e^{-\frac{\lambda^2}{4} - \lambda\sqrt{\rho(xt_1 + 1 - x)} - 4\rho x(1-x)q}. \quad (\text{E19})$$

Clearly, all the integrals are absolutely convergent for $D = 3$ and $q \neq 0$, thus one can set $D = 3$ and use the Mellin transform technique as before to obtain the small- q asymptotics. Direct calculation leads to

$$\sum_{i=1}^5 F_i(s) = -\frac{8}{15s^2} + \frac{8(15 \ln(4) - 46)}{225s} + \mathcal{O}(1), \quad (\text{E20})$$